Precise determination of the nonequilibrium tricritical point based on Lynden-Bell theory in the Hamiltonian mean-field model

Shun Ogawa* and Yoshiyuki Y. Yamaguchi†
Department of Applied Mathematics and Physics, Graduate School of Informatics, Kyoto University, 606-8501 Kyoto, Japan
(Received 10 June 2011; revised manuscript received 14 October 2011; published 22 December 2011)

Existence of a nonequilibrium tricritical point has been revealed in the Hamiltonian mean-field model by a nonequilibrium statistical mechanics. This statistical mechanics gives a distribution function containing unknown parameters, and the parameters are determined by solving simultaneous equations depending on a given initial state. Due to difficulty in solving these equations, pointwise numerical detection of the tricritical point has been unavoidable on a plane characterizing a family of initial states. In order to look into the tricritical point, we expand the simultaneous equations with respect to the order parameter and reduce them to one algebraic equation. The tricritical point is precisely identified by analyzing coefficients of the reduced equation. Reentrance to an ordered phase in a high-energy region is revisited around the obtained tricritical point.

DOI: 10.1103/PhysRevE.84.061140 PACS number(s): 05.70.Fh, 05.70.Jk, 05.20.−y

I. INTRODUCTION

Hamiltonian systems with long-range interactions [1,2] have several differences from ones with short-range interactions. One remarkable phenomenon in dynamics is that a system with long-range interactions is trapped in a long-lasting nonequilibrium quasi-stationary state (QSS) before it goes toward the thermal-equilibrium state. A lifetime of QSS diverges as the number N of particles increases. The divergence is observed as $N^{1.7}$ for a spatially homogeneous QSS [3,4] and as N^1 for an inhomogeneous QSS [5–8] in the Hamiltonian mean-field (HMF) model, and as $\ln N$ in the α-HMF model with $\alpha = 1$ [9], which corresponds to the boundary between long range and short range. Another typical time scaling is $N/\log N$ for stellar systems [10]. The divergence of lifetime implies that one can observe solely QSSs within his or her lifetime if the system size is large enough. Moreover, in QSSs, negative kinetic specific heat, whose temperature is associated with kinetic energy, possibly appears both in microcanonical and in canonical ensembles [11]. It is thus important to develop nonequilibrium statistical mechanics describing QSSs.

A QSS is recognized as a stable stationary solution to the Vlasov equation [2,3,10], which is also called the collisionless Boltzmann equation. The Vlasov description of N-body dynamics is verified if the mean-field approximation is appropriate [12–15]. The Vlasov equation admits continuous infinity of stationary states, and QSSs may depend on not only energy (or temperature) but also initial order parameter, for instance. A nonequilibrium statistical mechanics hence must determine a QSS for a given initial state.

Based on incompressibility of the Vlasov equation and the pioneering work of Lynden-Bell [16], a nonequilibrium statistical mechanics has been studied in a plasma system [17], in gravitating systems [18–21], and in the HMF model [22–24]. For plasma and gravitating systems, the nonequilibrium statistical mechanics is not a complete theory due to the appearance of the core-halo structure, but it is useful to describe QSSs in the HMF model, though the core-halo structure is also observed in the HMF model [25]. One of the remarkable predictions of the statistical theory is existence of first-order phase transition and a nonequilibrium tricritical point [24]. We stress that both the first-order phase transition and the tricritical point never appear in thermal equilibrium of the HMF model. Moreover, around the tricritical point, reentrant phenomenon to the ordered phase has been reported above the critical point [26], which is observed by N-body simulations. It is hence worth detecting the tricritical point on a parameter plane accurately, and investigating dynamics around the tricritical point.

The tricritical point has been detected as follows. The nonequilibrium statistical theory gives a Fermi-Dirac–type distribution function for a QSS, and the distribution function includes several undetermined variables depending on initial states. The undetermined variables are determined by solving simultaneous equations, which come from conservations holding in the Vlasov equation and the self-consistent condition for potential. After computing values of the undetermined variables, we divide the parameter plane into homogeneous (disordered) phase and inhomogeneous (ordered) phase, and draw transition lines as boundaries of the two phases. The tricritical point is found as the collapsing point between the second-order transition line and the first-order transition line.

Difficulty of detecting the tricritical point comes from complexity of the simultaneous equations, which include integrals of the Fermi-Dirac–type distribution function. One therefore has had to explore the parameter plane by pointwise numerical computations. The tricritical point sensitively depends on accuracy of computations [24,26], but the accuracy has been improved in a recent work [27].

Avoiding hard numerical computations to detect the position of the tricritical point accurately, we direct our attention to the fact that the order parameter is small enough around the second-order phase transition line, including the tricritical point. This fact admits to expand the simultaneous equations in power series with respect to the order parameter. Truncating simultaneous equations up to fifth order of the order parameter, we can reduce them into one algebraic equation of the order parameter whose coefficients depend on an initial state

*sogawa@amp.i.kyoto-u.ac.jp
†yyama@amp.i.kyoto-u.ac.jp

identified as a point on the parameter plane. The tricritical point is precisely detected by analyzing the coefficients with the aid of Landau's phenomenological theory. This method is much simpler than the method of solving the simultaneous equations used in the previous studies [24,26,27]. Around the obtained tricritical point, we revisit the reentrant phenomenon by performing N-body simulations.

We remark that there are two types of reentrant phenomenon around the tricritical point. One is predicted by the nonequilibrium statistical mechanics [22,26,27] by increasing energy with fixing the parameter representing the initial height of water-bag initial distribution. The other is observed numerically and is not theoretically predicted [26]. We will focus on the latter type of reentrant phenomenon by fixing the initial magnetization.

This article is constructed as follows. We review the Vlasov equation and Lynden-Bell's statistical theory quickly in Sec. II. The reduction of simultaneous equations is performed in Sec. III. The reduced equation is analyzed with the aid of Landau's phenomenological theory in Sec. IV. The reentrant phenomenon is revisited around the tricritical point in Sec. V. Section VI is devoted to summary and discussions.

II. VLASOV EQUATION AND LYNDEN-BELL'S THEORY

The considered model in this article is the HMF model whose Hamiltonian is written in the form

$$H_N = \sum_{i=1}^{N} \frac{{p_i}^2}{2} + \frac{1}{2N}\sum_{i,j=1}^{N}[1-\cos(\theta_i-\theta_j)],$$
$$\theta_i \in [-\pi,\pi], \quad p_i \in \mathbb{R}, \quad \text{for} \quad i=1,\ldots,N, \tag{1}$$

where N is the number of particles. The order parameter, or the magnetization, of this finite N-body system is defined as

$$M_x^{(N)} = \frac{1}{N}\sum_{i=1}^{N}\cos\theta_i, \quad M_y^{(N)} = \frac{1}{N}\sum_{i=1}^{N}\sin\theta_i,$$
$$M^{(N)} = |\vec{M}^{(N)}| = \sqrt{{M_x^{(N)}}^2 + {M_y^{(N)}}^2}. \tag{2}$$

This model has the homogeneous phase and the inhomogeneous phase, which are characterized by zero and nonzero modulus $M^{(N)}$ in the limit $N \to \infty$, respectively. The HMF model is one of the simplest models having long-range interactions, and its canonical equilibrium [28], thermodynamic stability [29], kinetic equation [30], dynamical stability [31] and Lyapunov instability, and finite size effects [32] have been investigated.

The N-body Hamiltonian dynamics is well described by the Vlasov equation,

$$\frac{\partial f}{\partial t} + p\frac{\partial f}{\partial \theta} - \frac{\partial \mathcal{H}[f]}{\partial \theta}\frac{\partial f}{\partial p} = 0, \tag{3}$$

in the large-N limit [12], where f is the one-body distribution function and $\mathcal{H}[f]$ is the one-body Hamiltonian defined by

$$\mathcal{H}[f] = \frac{p^2}{2} - \mathcal{M}_x[f]\cos\theta - \mathcal{M}_y[f]\sin\theta. \tag{4}$$

The order parameter vector $(\mathcal{M}_x[f],\mathcal{M}_y[f])$ in the Vlasov context is the continuous limit of $(M_x^{(N)},M_y^{(N)})$ [1,12,13] and is defined by

$$\mathcal{M}_x[f] = \int_{-\infty}^{+\infty} dp \int_0^{2\pi} f(\theta,p,t)\cos\theta\, d\theta, \tag{5}$$

$$\mathcal{M}_y[f] = \int_{-\infty}^{+\infty} dp \int_0^{2\pi} f(\theta,p,t)\sin\theta\, d\theta, \tag{6}$$

$$\mathcal{M}[f] = \sqrt{M_x[f]^2 + M_y[f]^2}. \tag{7}$$

QSSs are regarded as stable stationary solutions to the Vlasov equation [3]. It is, however, impossible to predict Vlasov equilibria dynamically for given initial states in general. We then use Lynden-Bell's pioneering idea of statistical mechanics, which takes incompressibility of the Vlasov dynamics into account [16].

We consider initial states which are two-valued water-bag distributions expressed by

$$f_0(\theta,p) = \begin{cases} f_0 & \text{for } (\theta,p) \in \mathcal{D}, \\ 0 & \text{otherwise}, \end{cases}$$
$$\mathcal{D} = [-\Delta\theta,\Delta\theta] \times [-\Delta p,\Delta p], \tag{8}$$
$$\Delta p \geqslant 0, \quad 0 \leqslant \Delta\theta \leqslant \pi.$$

The parameter f_0 is determined by the normalization condition as

$$f_0 = \frac{1}{4\Delta\theta\Delta p}. \tag{9}$$

The incompressibility implies exclusivity of area elements having the height f_0 on μ space, and leads the fermioniclike entropy [16],

$$\mathcal{S}[\bar{f}] = -\iint \left[\frac{\bar{f}}{f_0}\ln\frac{\bar{f}}{f_0} + \left(1-\frac{\bar{f}}{f_0}\right)\ln\left(1-\frac{\bar{f}}{f_0}\right)\right] d\theta\, dp, \tag{10}$$

where $\bar{f}(\theta,p)$ represents the coarse-grained distribution. In the following, we drop the bar of $\bar{f}$ for simplicity of the symbol. We stress that the parameter f_0, which reflects how particles spread in the μ space at the time $t=0$, appears explicitly in the entropy (10), so that the distribution function maximizing $\mathcal{S}[f]$ depends on the initial state.

We maximize the entropy (10) under the conservations of the normalization condition,

$$\mathcal{N}[f] = \iint f(\theta,p,t) d\theta\, dp = 1, \tag{11}$$

the total energy condition,

$$\mathcal{U}[f] = \iint \frac{p^2}{2} f(\theta,p,t) d\theta\, dp + \frac{1-(\mathcal{M}[f])^2}{2} = U, \tag{12}$$

and the total momentum condition,

$$\mathcal{P}[f] = \iint p f(\theta,p,t) d\theta\, dp = P. \tag{13}$$

Using Langrange multipliers, the variational problem is expressed as

$$\delta[\mathcal{S}[f] - \alpha(\mathcal{N}[f]-1) - \beta(\mathcal{U}[f]-U)$$
$$-\gamma(\mathcal{P}[f]-P)] = 0, \tag{14}$$

and the solution $f_{\rm LB}$ is

$$f_{\rm LB}(\theta,p) = \frac{f_0}{1+e^{\alpha+\beta(p^2/2-\mathcal{M}[f_{\rm LB}]\cos\theta)+\gamma p}}. \tag{15}$$

From the rotational symmetry of the HMF model, we set $\mathcal{M}_y[f]=0$ and wrote $\mathcal{M}_x[f]$ as $\mathcal{M}[f]$ without loss of generality.

The distribution function (15) has four undetermined variables: the three Lagrange multipliers α,β,γ and the magnetization $\mathcal{M}[f_{\rm LB}]$. The magnetization $\mathcal{M}[f_{\rm LB}]$ must satisfy the self-consistent equation

$$\mathcal{M}[f_{\rm LB}] = \iint f_{\rm LB}(\theta,p)\cos\theta\, d\theta\, dp = M. \tag{16}$$

For the water-bag initial state (8), the total momentum P takes 0 and hence γ is 0. The distribution function hence becomes

$$f_{\rm LB}(\theta,p) = \frac{f_0}{1+e^{\alpha+\beta(p^2/2-M\cos\theta)}}. \tag{17}$$

The undetermined parameters α, β, and M are determined by solving three equations (11), (12), and (16), simultaneously for a given initial state parametrized by the pair of $(\Delta\theta,\Delta p)$. This pair gives the initial magnetization,

$$M_0 = \frac{\sin\Delta\theta}{\Delta\theta}, \tag{18}$$

and the energy U,

$$U = \frac{(\Delta p)^2}{6} + \frac{1-(M_0)^2}{2}, \tag{19}$$

and hence initial states are also parametrized by the pair of (M_0,U) instead of $(\Delta\theta,\Delta p)$. We use the former pair.

Solving the simultaneous equations is the most difficult step in determining the distribution function and drawing the phase diagram on the parameter plane (M_0,U). This is the reason why we need a theoretical reduction of the simultaneous equations.

III. REDUCTION OF SIMULTANEOUS EQUATIONS

The idea to reduce the simultaneous equations is to expand them into power series of the order parameter M by focusing on the fact that M is small around the second-order phase transition line. The strategy is as follows. We obtain α and β as functions of M by expanding two equations $\mathcal{N}[f_{\rm LB}]=1$ and $\mathcal{U}[f_{\rm LB}]=U$ with respect to M and by solving them up to the fifth order of M. Substituting the obtained α and β into expansion of the equation $\mathcal{M}[f_{\rm LB}]=M$, we have one algebraic equation of M. One solution to the algebraic equation gives one value of magnetization M, and M gives α and β accordingly. The obtained distribution function $f_{\rm LB}$ corresponds to a QSS if it is stable. Roughly speaking, the phase diagram is drawn on the parameter plane (M_0,U) by counting the number of solutions of M.

A. Elimination of β

We can extract β from integrands of the simultaneous equations by changing variables as $x=p\sqrt{\beta/2}$ and $\eta=\beta M$. The transformed simultaneous equations are

$$f_0\left(\frac{2}{\beta}\right)^{1/2} F(\alpha,\eta) = 1, \tag{20}$$

$$f_0\left(\frac{2}{\beta}\right)^{3/2} G(\alpha,\eta) = 2U-1+\frac{\eta^2}{\beta^2}, \tag{21}$$

$$f_0\left(\frac{2}{\beta}\right)^{1/2} H(\alpha,\eta) = \frac{\eta}{\beta}, \tag{22}$$

where the functions F, G, and H are defined by

$$F(\alpha,\eta) = \int_{-\infty}^{\infty}dx\int_0^{2\pi}\frac{d\theta}{1+e^{\alpha-\eta\cos\theta+x^2}} \tag{23}$$

$$G(\alpha,\eta) = \int_{-\infty}^{\infty}dx\int_0^{2\pi}\frac{x^2 d\theta}{1+e^{\alpha-\eta\cos\theta+x^2}}, \tag{24}$$

$$H(\alpha,\eta) = \int_{-\infty}^{\infty}dx\int_0^{2\pi}\frac{\cos\theta\, d\theta}{1+e^{\alpha-\eta\cos\theta+x^2}}. \tag{25}$$

We remark that F and G are even with respect to η, and H odd:

$$\begin{aligned} F(\alpha,-\eta) &= F(\alpha,\eta),\\ G(\alpha,-\eta) &= G(\alpha,\eta),\\ H(\alpha,-\eta) &= -H(\alpha,\eta). \end{aligned} \tag{26}$$

The normalization condition (20) gives

$$\sqrt{\beta} = \sqrt{2} f_0 F(\alpha,\eta), \tag{27}$$

and, using Eq. (27), we can eliminate β from energy condition (21) and the self-consistent equation (22) as

$$F(\alpha,\eta)G(\alpha,\eta) = f_0^2(2U-1)F(\alpha,\eta)^4 + \frac{\eta^2}{4f_0^2}, \tag{28}$$

$$F(\alpha,\eta)H(\alpha,\eta) = \frac{\eta}{2f_0^2}, \tag{29}$$

respectively.

B. Determination of $\alpha(\eta)$

We assume that $|\eta|\ll 1$, and solve Eq. (28) with respect to α. This assumption requires that both M and β are small, and breaks around $M_0\simeq 0$, since β becomes large. The solved α, denoted by $\alpha(\eta)$, must be even with respect to η thanks to the fact of Eq. (26). See the Appendix for details. The solution $\alpha(\eta)$ is hence expanded as

$$\alpha(\eta) = \alpha_0 + \alpha_2\eta^2 + \alpha_4\eta^4 + \alpha_6\eta^6 + \cdots. \tag{30}$$

Substituting the expansion (30) into $F(\alpha,\eta)$, we get

$$\begin{aligned} F(\alpha(\eta),\eta) = {}& F_0(\alpha_0) + F_2(\alpha_0,\alpha_2)\eta^2\\ &+ F_4(\alpha_0,\alpha_2,\alpha_4)\eta^4 + \cdots, \end{aligned} \tag{31}$$

where

$$F_0(\alpha_0) = F(\alpha_0,0), \tag{32}$$

$$F_2(\alpha_0,\alpha_2) = F_\alpha(\alpha_0,0)\alpha_2 + \tfrac{1}{2}F_{\eta\eta}(\alpha_0,0), \tag{33}$$

$$F_4(\alpha_0,\alpha_2,\alpha_4) = F_\alpha(\alpha_0,0)\alpha_4 + \frac{1}{2}F_{\alpha\alpha}(\alpha_0,0)\alpha_2^2 + \frac{1}{2}F_{\alpha\eta\eta}(\alpha_0,0)\alpha_2 + \frac{1}{4!}F_{\eta\eta\eta\eta}(\alpha_0,0). \quad (34)$$

The symbol $F_{\alpha\eta\eta}$, for instance, denotes that

$$F_{\alpha\eta\eta} = \frac{\partial^3 F}{\partial\alpha\partial\eta^2}. \quad (35)$$

The expansion of G is obtained by replacing F with G in the above expressions. Considering Eq. (28) in each order of η, we obtain the equations for α_0, α_2, and α_4 as

$$F_0G_0 - f_0^2(2U-1)F_0^4 = 0, \quad (36)$$

$$F_0G_2 + F_2G_0 - 4f_0^2(2U-1)F_0^3F_2 - \frac{1}{4f_0^2} = 0, \quad (37)$$

$$F_0G_4 + F_2G_2 + F_4G_0 - f_0^2(2U-1)\big(6F_0^2F_2^2 + 4F_0^3F_4\big) = 0, \quad (38)$$

respectively. The value of α_0 is determined by solving Eq. (36), which depends on α_0 only. The value of α_2 is determined by solving Eq. (37), and we get

$$\alpha_2 = \frac{1 - 2f_0^2(FG_{\eta\eta} - 3F_{\eta\eta}G)}{4f_0^2(FG_\alpha - 3F_\alpha G)}, \quad (39)$$

where the functions of the right-hand side are evaluated at $(\alpha,\eta) = (\alpha_0,0)$. The value of α_4 is computed from the relation

$$\begin{aligned} -F(FG_\alpha - 3F_\alpha G)\alpha_4 &= \left[\frac{1}{2}F(FG_{\alpha\alpha} - 3F_{\alpha\alpha}G) + F_\alpha(FG_\alpha - 6F_\alpha G)\right]\alpha_2^2 \\ &+ \left[\frac{1}{2}F(FG_{\alpha\eta\eta} - 3F_{\alpha\eta\eta}G) + \frac{1}{2}F(F_\alpha G_{\eta\eta} + F_{\eta\eta}G_\alpha) - 6F_\alpha F_{\eta\eta}G\right]\alpha_2 + \left[\frac{1}{4!}F(FG_{\eta\eta\eta\eta} - 3F_{\eta\eta\eta\eta}G) \right.\\ &\left. + \frac{1}{4}F_{\eta\eta}(FG_{\eta\eta} - 6F_{\eta\eta}G)\right]. \end{aligned} \quad (40)$$

The functions appearing in Eq. (40) are evaluated at $(\alpha,\eta) = (\alpha_0,0)$ again. The solution $\alpha(\eta)$ is hence obtained by Eqs. (36), (39), and (40) up to $O(\eta^5)$.

C. Reduced equation

Remembering that the function $H(\alpha,\eta)$ is odd with respect to η, we can expand $H(\alpha(\eta),\eta)$ as

$$H(\alpha(\eta),\eta) = H_1(\alpha_0)\eta + H_3(\alpha_0,\alpha_2)\eta^3 + H_5(\alpha_0,\alpha_2,\alpha_4)\eta^5 + \cdots, \quad (41)$$

where

$$H_1(\alpha_0) = H_\eta(\alpha_0,0), \quad (42)$$

$$H_3(\alpha_0,\alpha_2) = H_{\alpha\eta}(\alpha_0,0)\alpha_2 + \frac{1}{3!}H_{\eta\eta\eta}(\alpha_0,0), \quad (43)$$

$$H_5(\alpha_0,\alpha_2,\alpha_4) = H_{\alpha\eta}(\alpha_0,0)\alpha_4 + \frac{1}{2}H_{\alpha\alpha\eta}(\alpha_0,0)\alpha_2^2 + \frac{1}{3!}H_{\alpha\eta\eta\eta}(\alpha_0,0)\alpha_2 + \frac{1}{5!}H_{\eta\eta\eta\eta\eta}(\alpha_0,0). \quad (44)$$

Substituting the expansions of F and H, Eqs. (31) and (41), respectively, into the self-consistent equation (29), we obtain the reduced equation in η as

$$\tilde{A}\eta + \tilde{B}\eta^3 + \tilde{C}\eta^5 + O(\eta^7) = 0, \quad (45)$$

where

$$\tilde{A} = \frac{1}{2f_0^2} - F_0(\alpha_0)H_1(\alpha_0), \quad (46)$$

$$\tilde{B} = -\left[F_0(\alpha_0)H_3(\alpha_0,\alpha_2) + F_2(\alpha_0,\alpha_2)H_1(\alpha_0)\right], \quad (47)$$

$$\tilde{C} = -[F_0(\alpha_0)H_5(\alpha_0,\alpha_2,\alpha_4) + F_2(\alpha_0,\alpha_2)H_3(\alpha_0,\alpha_2) + F_4(\alpha_0,\alpha_2,\alpha_4)H_1(\alpha_0)]. \quad (48)$$

The reduced equation (45) is written in η, but what we have to compute is a reduced equation in M. For rewriting Eq. (45) into the power series of M, we expand β as a series of η as

$$\beta(\eta) = 2f_0^2F(\alpha(\eta),\eta)^2 = \beta_0 + \beta_2\eta^2 + \beta_4\eta^4 + \cdots, \quad (49)$$

where

$$\beta_0 = 2f_0^2F_0(\alpha_0)^2, \quad (50)$$

$$\beta_2 = 4f_0^2F_0(\alpha_0)F_2(\alpha_0,\alpha_2), \quad (51)$$

$$\beta_4 = 2f_0^2[2F_0(\alpha_0)F_4(\alpha_0,\alpha_2,\alpha_4) + F_2(\alpha_0,\alpha_2)^2]. \quad (52)$$

We used the fact that $\beta(\eta)$ is even, since $F(\alpha(-\eta),-\eta) = F(\alpha(\eta),\eta)$. Substituting the definition $\eta = \beta M$ into Eq. (49) recursively, we get

$$\beta = \beta_0 + \beta_0^2\beta_2M^2 + \beta_0^3\big(\beta_0\beta_4 + 2\beta_2^2\big)M^4 + O(M^6), \quad (53)$$

and the reduced equation (45) is rewritten in the form

$$AM + BM^3 + CM^5 + O(M^7) = 0, \quad (54)$$

where

$$A = \beta_0\tilde{A}, \quad (55)$$

$$B = \beta_0^2(\tilde{A}\beta_2 + \tilde{B}\beta_0), \quad (56)$$

$$C = \beta_0^3\big[\tilde{A}\big(\beta_0\beta_4 + 2\beta_2^2\big) + 3\tilde{B}\beta_0\beta_2 + \tilde{C}\beta_0^2\big]. \quad (57)$$

Note that A, B, and C depend on f_0 and U only, and we can compute their values from a given initial state characterized by (f_0,U) or (M_0,U). Equation (54) is odd with respect to M, and $-M$ is a solution if M is. The number of real solutions is hence 1, 3, or 5 if we neglect $O(M^7)$, and the number depends on signs of the coefficients A, B, and C. For each of the solutions M, values of α and β, and hence the distribution function (17), are determined from the expansions (30) and (49) by using the definition $\eta = \beta M$ up to $O(\eta^5)$.

IV. LANDAU'S PHENOMENOLOGICAL THEORY

It is helpful to introduce the pseudo free energy $\Psi(M)$, whose critical points represent (meta)equilibrium states. A critical point of $\Psi(M)$ is stable (unstable) if it is a local minimum (maximum) point. Phase transitions occur when the minimum point of $\Psi(M)$ changes from $M = 0$ to $M \neq 0$. Analysis of phase transitions by using the pseudo free energy is called Landau's phenomenological theory [33]. For reproducing the reduced equation (54) as a derivative of the pseudo free energy, we define $\Psi(M)$ by

$$\Psi(M) = \Psi_0 + \frac{A}{2}M^2 + \frac{B}{4}M^4 + \frac{C}{6}M^6 + O(M^8). \quad (58)$$

We note that both $\Psi(M)$ and $-\Psi(M)$ give the same equation for obtaining the critical points, but stability is opposite between the two. The signature of pseudo free energy is determined by noting that the coefficient A can be rewritten,

$$A = \frac{\beta_0}{f_0^2}\left[1 + \pi \int_{-\infty}^{\infty} \frac{1}{p}\frac{df_{\mathrm{LB,hom}}}{dp}(p)dp\right], \quad (59)$$

where $f_{\mathrm{LB,hom}}$ is a homogeneous Lynden-Bell distribution function defined by replacing α with α_0, β with β_0, and setting $M = 0$ in Eq. (17). The inside of the brace in Eq. (59), denoted by I, represents linear [31,34,35] and formal stability [3] of the homogeneous state $f_{\mathrm{LB,hom}}$, and $I > 0$ ($I < 0$) implies that $f_{\mathrm{LB,hom}}$ is stable (unstable). The equation $I = 0$ has been used for obtaining the stability diagram of the homogeneous Lynden-Bell distribution function [22]. From the facts $F_0(\alpha_0) > 0$ and hence $\beta_0 > 0$, the signature of A is identical with I and hence $A > 0$ implies that $f_{\mathrm{LB,hom}}$ is stable. On the other hand, positive A implies that a solution $M = 0$ to $d\Psi/dM = 0$ is a local minimum point, and hence the pseudo free energy must be $\Psi(M)$ instead of $-\Psi(M)$.

Landau's phenomenological theory gives a phase diagram on the (A,B) plane by assuming that C is always positive. The lines $A = 0$ for $B > 0$ and $3B^2 - 16AC = 0$ for $B < 0$ represent second- and first-order phase transition lines, respectively. The coexistence region associated to the first-order phase transition is bounded by $A = 0$ and $B^2 - 4AC = 0$. The three lines $A = 0, 3B^2 - 16AC = 0$, and $B^2 - 4AC = 0$ meet at the origin $A = B = 0$, and the tricritical point is located at the meeting point [36]. We stress that the condition $A = B = 0$ is exact to detect the tricritical point, since five solutions to Eq. (54) are degenerated at $M = 0$ irrespective of neglected higher-order terms.

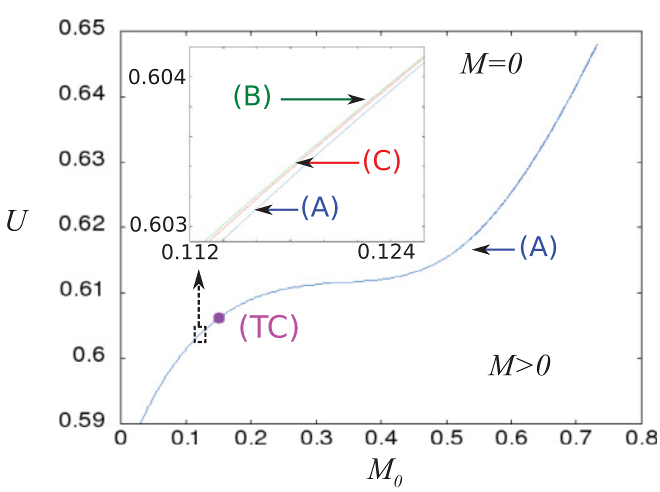

FIG. 1. (Color online) Phase diagram on the parameter plane (M_0,U). Lines (A), (B), and (C) represent $A = 0, 3B^2 - 16AC = 0$, and $B^2 - 4AC = 0$, respectively. The point (TC) represents the tricritical point. The region enclosed by lines (A) and (B) is the coexistence region. The ordered and the disordered phases appear in the lower side of (B) and the upper side of (A), respectively.

TABLE I. Comparison of values of parameters at points which are reported as the tricritical point in the present and a previous paper [27].

	U^{tc}	M_0^{tc}	f_0^{tc}
Present result	0.606178	0.15118	0.10949
Result in Ref. [27]	0.6059	0.15	0.109497

The coefficients A,B depend on f_0 and U through α_0 and α_2, and the phase diagram on the (A,B) plane can be mapped to the (M_0,U) plane. We remark that C is always positive around the phase transition lines according to numerical computations. The obtained phase diagram is shown in Fig. 1, which is qualitatively consistent with the previously reported one in Ref. [24]. We denote the values of U, M_0, and f_0 by U^{tc}, M_0^{tc}, and f_0^{tc}, respectively, at the tricritical point. The values arranged in Table I are in good agreement with the values reported in [27].

V. N-BODY SIMULATIONS

Results of nonequilibrium statistical mechanics are supported by N-body simulations in a region which is not close to the tricritical point [24]. Around the tricritical point, however, a discrepancy between the statistical mechanics and N-body simulations has been reported in Ref. [26]. The statistical mechanics predicts monotonically decreasing M as a function of energy U, but N-body simulations have revealed a reentrance to an inhomogeneous phase in a high-energy region in the (M_0,U) plane. We revisit this reentrant phenomenon around the obtained exact tricritical point. To avoid confusion, we again stress that this reentrant phase corresponds to what is called "the second (unexpected) reentrant phase" in Fig. 12 of Ref. [26].

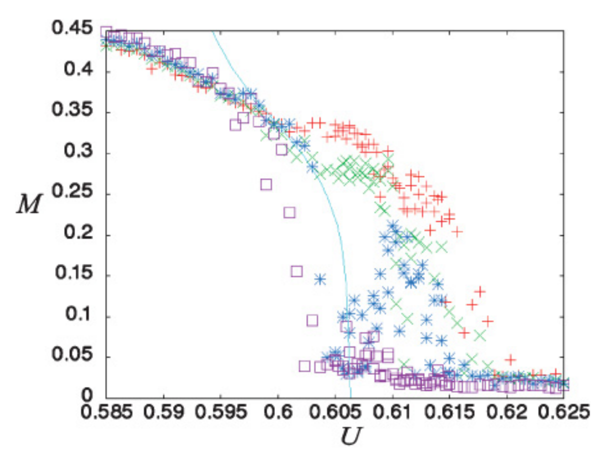

FIG. 2. (Color online) Energy dependences of magnetization for four fixed values of M_0 around M_0^{tc}. $M_0 = 0.10$ (□), M_0^{tc} ($*$), 0.18 ($\times$), and 0.20 (+). The number of particles N is 10^5. Points are obtained by taking averages over time from $t = 500$ to $t = 1000$. The solid line is obtained by using the Landau theory for M_0^{tc}. We remark that validity of the Landau theory is not guaranteed for large M.

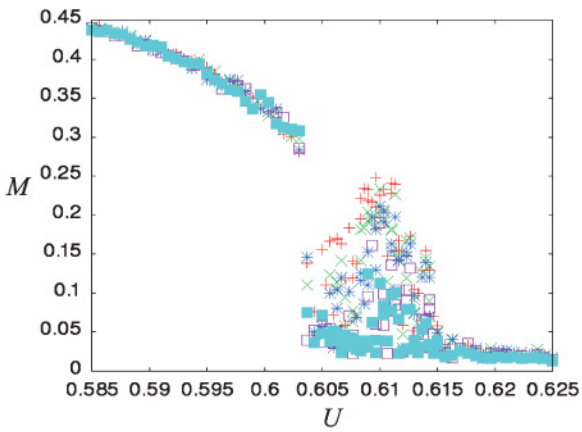

FIG. 3. (Color online) Same as Fig. 2, but for $M_0 = 0.13$ (■), 0.14 (□), $M_0^{\rm tc}$ ($*$), 0.155 ($\times$), and 0.16 (+).

The canonical equation derived from the Hamiltonian of the HMF model is written in the form

$$\frac{d\theta_i}{dt} = p_i, \quad \frac{dp_i}{dt} = -M_x^{(N)} \sin\theta_i + M_y^{(N)} \cos\theta_i, \qquad (60)$$

for $i = 1, \dots, N$. We integrate the equation of motion (60) numerically by using a fourth-order symplectic integrator [37] with step size $dt = 0.1$. Initial values of θ_i and p_i are randomly drawn from the water-bag distribution (8).

We investigate the reentrant phenomenon by changing value of M_0 around the tricritical value $M_0^{\rm tc}$. The results of N-body simulations are reported in Figs. 2 and 3. According to the statistical theory, increasing M_0, the order of the phase transition changes from first to second when the initial order parameter passes $M_0^{\rm tc}$. It is also predicted that the transition energy $U^{\rm c}(M_0)$ should vary continuously when M_0 crosses $M_0^{\rm tc}$. This is however not supported by N-body simulations. A schematic picture of energy dependences of magnetization is illustrated for several values of M_0 in Fig. 4. As M_0 increases, the reentrant phenomenon becomes clearer in one side, $M_0 < M_0^{\rm tc}$, but it tends to disappear in the other side, $M_0 > M_0^{\rm tc}$.

To show the signalization of the reentrance around the tricritical value $M_0^{\rm tc}$ clearly, the local maximum and the local

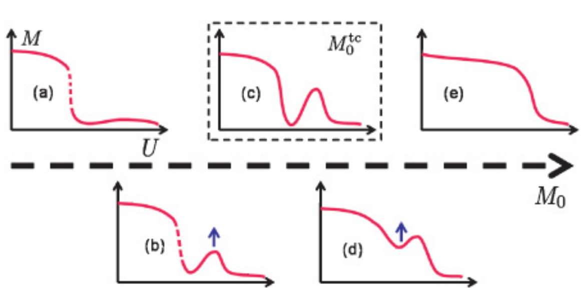

FIG. 4. (Color online) Schematic picture of energy dependences of magnetization. Broken lines in (a) and (b) represent jumps due to the first-order phase transitions, which are predicted by the statistical mechanics [24]. Two upper arrows in (b) and (d) represent direction of change by increasing the initial magnetization M_0. A reentrant phenomenon appears and grows (b), and the growth stops at the tricritical value $M_0^{\rm tc}$ (c). The panel (d) is for the value of $M_0 \sim 0.18$. The reentrance disappears in large values of M_0 (e).

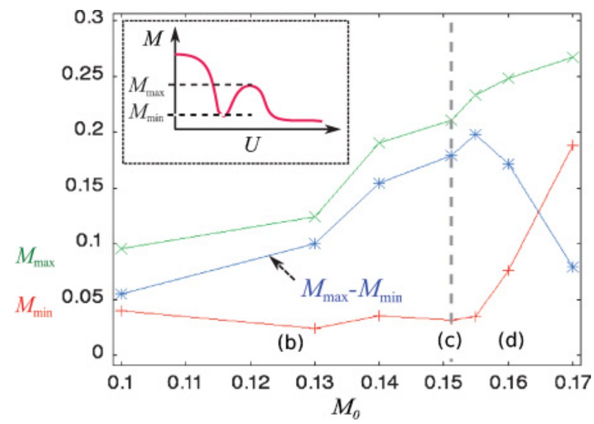

FIG. 5. (Color online) Local maximum $M_{\rm max}$ ($\times$), the local minimum $M_{\rm min}$ (+), and their difference $M_{\rm max} - M_{\rm min}$ ($*$) as functions of M_0. $M_{\rm max}$ and $M_{\rm min}$ are defined in the inset. This graph is obtained from the results exhibited in Figs. 2 and 3. The values of M_0 marked by (b), (c), and (d) in this figure correspond to panels (b), (c), and (d) of Fig. 4, respectively.

minimum, which are observed in panels (b), (c), and (d) of Fig. 4, are reported as functions of M_0 in Fig. 5. The $M_{\rm max} - M_{\rm min}$ takes the maximum value around $M_0 = 0.155$, which is close to $M_0^{\rm tc}$ within 3% error. This error is compatible with the error of the tricritical point, which is observed by M_0 dependence of M with the fixed energy value $U = U^{\rm tc}$, though it is not reported. We may therefore conclude that the reentrant phenomenon is signalized around the tricritical point.

VI. SUMMARY

A tricritical point has been reported on a parameter plane associated to a family of water-bag initial states in the HMF model. One water-bag initial state goes to a Lynden-Bell distribution, which has three undetermined variables, and the three variables, including the order parameter, are determined by solving three simultaneous equations. Due to difficulty in this solving step, pointwise numerical detection of the position of the tricritical point has been unavoidable.

We overcame this pointwise detection by deriving one reduced equation for the order parameter by expanding the three simultaneous equations with respect to the order parameter. One solution to the reduced equation gives magnetization in a QSS for a given initial state, which is represented as a point on a two-dimensional parameter plane. The phase diagram on the parameter plane is hence drawn by analyzing the coefficients of the reduced equation, since the coefficients are functions on the parameter plane. We remark that the coefficient of the leading order is equivalent to the formal and linear stability criterion for homogeneous stationary states [3,35], and zero level contour of this coefficient corresponds to the order-disorder transition. The obtained phase diagram is qualitatively in good agreement with ones previously obtained by directly solving the three simultaneous equations [24,26,27]. Furthermore, the tricritical point detected in the present paper is in good agreement with that obtained by the detailed investigation reported in Ref. [27].

We emphasize that the obtained tricritical point is theoretically exact, since the assumption of the present method is that the product of the order parameter and the inverse temperature is small enough and is satisfied around the tricritical point. Potential importance of the present method is that it is applicable to other statistical theories and systems, if order parameters explicitly appear in smooth one-body distributions.

One statistical theory has been proposed based on the core-halo structure [25], and the core-halo theory gives a different phase diagram from one given by the Lynden-Bell theory. For applying the present method to the core-halo theory, we need to solve two problems: One is that the core-halo theory includes a parameter determined with the aid of a numerical simulation, and an extended theory is necessary to determine the parameter theoretically. The other is that a distribution function in the core-halo theory is expressed by step functions, which are not smooth and are not expanded in the Taylor series. It might be worth exploring the phase diagram based on the core-halo theory theoretically by overcoming these difficulties.

Around the obtained tricritical point, we revisited the reentrant phenomenon, which is not a theoretically predicted type [22,26,27] along iso-f_0 lines, but is a numerically observed type [26]. The latter type appears even along iso-M_0 lines, and we explicitly confirmed the appearance of this type of reentrance by performing N-body simulations. An important observation by our computations is that the reentrant phenomenon is signalized around the tricritical point. The origin of this type of reentrant phenomenon is still unclear, and is an open problem.

ACKNOWLEDGMENTS

The authors would like to thank Stefano Ruffo for fruitful discussions and Toshihiro Iwai for his comments on this study. The authors also appreciate comments of anonymous referees to improve the present paper. S.O. has been supported by the Kyoto University Global COE Program: Informatics Education and Research Center for Knowledge-Circulating Society. Y.Y.Y. has been supported by Grant-in-Aid for Scientific Research (C), 23560069.

APPENDIX: EVENNESS OF α

Let us introduce a function $K(\alpha,\eta)$ defined by

$$K(\alpha,\eta) = F(\alpha,\eta)G(\alpha,\eta) - f_0^2(2U-1)F(\alpha,\eta)^4 - \frac{\eta^2}{4f_0^2}. \tag{A1}$$

This function K is even with respect to η, and we can expand K as

$$K(\alpha,\eta) = \sum_{n=0}^{\infty} \frac{\partial^{2n}K}{\partial\eta^{2n}}(\alpha,0)\frac{\eta^{2n}}{(2n)!}, \tag{A2}$$

where $0! = 1$. We solve $K(\alpha,\eta) = 0$ with respect to α, and show that the solution $\alpha(\eta)$ is even under some assumptions.

We expand the solution $\alpha(\eta)$ as

$$\alpha(\eta) = \alpha_0 + \sum_{m=1}^{\infty} \alpha_m \eta^m. \tag{A3}$$

Substituting this expansion (A3) into Eq. (A2), we have

$$K(\alpha(\eta),\eta) = \sum_{n=0}^{\infty}\sum_{k=0}^{\infty} \frac{1}{(2n)!k!}\frac{\partial^{2n+k}K}{\partial\alpha^k\partial\eta^{2n}}(\alpha_0,0) \times \left[\sum_{m=1}^{\infty}\alpha_m\eta^m\right]^k \eta^{2n}. \tag{A4}$$

The condition $K(\alpha(\eta),\eta) = 0$ implies that the coefficient must vanish in each order of η. From the terms of $O(\eta)$, which comes from $n = 0$ and $k = 1$, we get $\alpha_1 = 0$ if $(\partial K/\partial\alpha)(\alpha_0,0) \neq 0$. The terms of $O(\eta^3)$ are proportional to α_1 or α_3, and α_3 appears only in the term

$$\frac{\partial K}{\partial\alpha}(\alpha_0,0)\alpha_3\eta^3, \tag{A5}$$

which comes from $n = 0$ and $k = 1$. The coefficient α_1 vanishes and hence $\alpha_3 = 0$ if $(\partial K/\partial\alpha)(\alpha_0,0) \neq 0$. Similarly, we can prove that $\alpha_{2l+1} = 0$ from the facts that (i) each $O(\eta^{2l+1})$ term includes one odd number of $\alpha_m (m \leqslant 2l+1)$ at least, (ii) $\alpha_m = 0$ for $m = 1,3,\ldots,2l-1$, and (iii) α_{2l+1} comes from $n = 0$, $k = 1$, and $m = 2l+1$, which gives only the term

$$\frac{\partial K}{\partial\alpha}(\alpha_0,0)\alpha_{2l+1}\eta^{2l+1}. \tag{A6}$$

Consequently, if $(\partial K/\partial\alpha)(\alpha_0,0) \neq 0$ at the $\alpha = \alpha_0$, which satisfies $K(\alpha_0,0) = 0$, then $\alpha(\eta)$ is even.

The above function $\partial K/\partial\alpha$ is estimated at $\eta = \beta M = 0$, which implies $M = 0$ for finite temperature. Using $M = 0$, the one-body Hamiltonian $\mathcal{H}[f]$ (4) is positive and hence the chemical potential $\mu = -\alpha/\beta$ is positive accordingly. Consequently, the parameter α is negative. Numerical computations reveal that $\partial K/\partial\alpha$ is negative for negative α, and the assumption $(\partial K/\partial\alpha)(\alpha_0,0) \neq 0$ is satisfied in the HMF model.

[1] A. Campa, T. Dauxois, and S. Ruffo, Phys. Rep. **480**, 57 (2009).
[2] T. Daxois, S. Ruffo, E. Arimond, and M. Wilkens, *Dynamics and Thermodynamics of Systems with Long-Range Interactions*, Lecture Notes in Physics (Springer, Berlin, 2002).
[3] Y. Y. Yamaguchi, J. Barré, F. Bouchet, T. Dauxois, and S. Ruffo, Physica A **337**, 36 (2004).
[4] J. Barré, F. Bouchet, T. Dauxois, S. Ruffo, and Y. Y. Yamaguchi, Physica A **365**, 177 (2006).
[5] P. de Buyl, D. Mukamel, and S. Ruffo, e-print arXiv:1012.2594.
[6] P. H. Chavanis, Physica A **377**, 469 (2007).
[7] P. H. Chavanis, J. Stat. Mech. (2010) P05019.
[8] P. H. Chavanis, e-print arXiv:1107.1475.
[9] A. Turchi, D. Fanelli, and X. Leoncini, Commun. Nonlinear Sci. Numeric. Sim. **16**, 4718 (2011).
[10] J. Binney and S. Tremaine, *Galactic Dynamics* (Princeton University Press, Princeton, NJ, 1987).

[11] F. Staniscia, A. Turchi, D. Fanelli, P. H. Chavanis, and G. De Ninno, Phys. Rev. Lett. **105**, 010601 (2010).
[12] W. Braun and K. Hepp, Commun. Math. Phys. **56**, 101 (1977).
[13] H. Spohn, *Large Scale Dynamics of Interacting Particles* (Springer-Verlag, Heidelberg, 1991).
[14] E. M. Lifshitz and L. P. Pitaevski, *Physical Kinetics* (Pergamon Press, New York, 1981).
[15] N. Pottier, *Non-equilibrium Statistical Physics Linear Irreversible Processes* (Oxford University Press, New York, 2010).
[16] D. Lynden-Bell, Mon. Not. R. Astron. Soc. **136**, 101 (1967).
[17] Y. Levin, R. Pakter, and T. N. Teles, Phys. Rev. Lett. **100**, 040604 (2008).
[18] P. H. Chavanis and J. Sommeria, Mon. Not. R. Astron. Soc. **269**, 569 (1998).
[19] Y. Levin, R. Pakter, and F. B. Rizzato, Phys. Rev. E **78**, 021130 (2008).
[20] Y. Y. Yamaguchi, Phys. Rev. E **78**, 041114 (2008).
[21] M. Joyce and T. Worrakitpoonpon, Phys. Rev. E **84**, 011139 (2011).
[22] P. H. Chavanis, Eur. Phys. J. B **53**, 487 (2006).
[23] A. Antoniazzi, D. Fanelli, J. Barré, P. H. Chavanis, T. Dauxois, and S. Ruffo, Phys. Rev. E **75**, 011112 (2007).
[24] A. Antoniazzi, D. Fanelli, S. Ruffo, and Y. Y. Yamaguchi, Phys. Rev. Lett. **99**, 040601 (2007).
[25] R. Pakter and Y. Levin, Phys. Rev. Lett. **106**, 200603 (2011).
[26] F. Staniscia, P. H. Chavanis, G. De Ninno, and D. Fanelli, Phys. Rev. E **80**, 021138 (2009).
[27] F. Staniscia, P. H. Chavanis, and G. De Ninno, Phys. Rev. E **83**, 051111 (2011).
[28] M. Antoni and S. Ruffo, Phys. Rev. E **52**, 2361 (1995).
[29] S. Inagaki, Prog. Theor. Phys. **90**, 577 (1993).
[30] S. Inagaki, Prog. Theor. Phys. **96**, 1307 (1996).
[31] S. Inagaki and T. Konishi, Publ. Astron. Soc. Jpn. **45**, 733 (1993).
[32] V. Latora, A. Rapisarda, and S. Ruffo, Phys. Rev. Lett. **80**, 692 (1998).
[33] L. D. Landau and E. M. Lifshitz, *Statistical Physics* (Pergamon Press, New York, 1968).
[34] O. Penrose, Phys. Fluids **3**, 258 (1960).
[35] P. H. Chavanis and L. Delfini, Eur. Phys. J. B **69**, 389 (2009).
[36] H. Nishimori and G. Ortiz, *Elements of Phase Transitions and Critical Phenomena* (Oxford University Press, New York, 2011).
[37] H. Yoshida, Celest. Mech. Dynam. Astron. **56**, 27 (1993).